The influence of stress-induced anisotropy in undrained yield and ultimate shear strengths in brittle loose deposited silts

António Viana da Fonseca[1#], *Fausto* Molina-Gómez[1], *Davide* Besenzon[1,2] and *Daniela* Coelho[3]

[1]*CONSTRUCT-GEO, Universidade do Porto (FEUP), Rua Dr. Roberto Frias s/n, Porto, Portugal*
[2] *Escuela Superior Politécnica Del Litoral (ESPOL-FICT), Campus Gustavo Galindo, Guayaquil, Equador*
[3]*Faculdade de Engenharia, Universidade do Porto (FEUP), Rua Dr. Roberto Frias s/n, Porto, Portugal*
[#]*Corresponding author: viana@fe.up.pt*

ABSTRACT

The typical undrained behaviour observed in brittle non-plastic soil is ruled by the combination of density and stress levels. Some specific silty and sandy mining waste with particles morphologies that generate high small-strain stiffness to strength ratios when increasing deviatoric stress (q) in stress paths that tend to decrease mean effective stress ($p´$) may drop down the deviatoric stress before reaching the frictional critical sate. The ratio between the peak (or yield) value (S_u=q/2) and the corresponding $p´$ is usually associated with a locus in q-$p´$ that is commonly associated to a straight Instability Line (I_L) with a unique ratio (η_{IL}) and for an initial state parameter. However, this is not the case if an induced anisotropy is installed differently while the at rest stress ratio (hereby defined as initial, K_0) is achieved by continuous rate the principal stresses consolidated in lab prior to loading with distinct values. This fabric effect is decisive for design and in stability assessment of earth structures, like dams or piles of mine tailings where non-plastic fines are dominant, even if the prevailing stress-path is in compression. In a thorough and quite complete program varying these conditions on iron ore tailings from Minas Gerais state in Brazil, reconstituted in lab with differentiated state parameters, and its relation to the induced anisotropy effect.

Keywords: Tailings from iron ore mining; liquefiable soils; peak or yield undrained strength; residual or ultimate undrained strength

1. Introduction

Recent dam failures have highlighted the brittleness of the materials deposited in Tailings Storage Facilities (TSF), especially dams, emphasising the importance of studying these peculiar materials to understand their hydro-mechanical behaviour for safer designing. The tailings Dam I at the Córrego do Feijão iron mine complex (Brumadinho, MG, Brazil) collapsed in January 2019 due to liquefaction. An extensive laboratory testing campaign included a large number of triaxial tests, on remoulded samples of 4 types (clusters) of deposited tailings –all with different percentages of iron elements– to define constitutive parameters for numerical simulation of the failure using a constitutive model (CASM). The tests were carried out under diverse initial state conditions (loose and dense), consolidation paths (isotropic and anisotropic) and shear paths (drained and undrained; compression and extension under strain and stress control) as reported by Viana da Fonseca et al. (2022a) and Viana da Fonseca et al. (2022b).

The test results embraced the evaluation of physical, hydraulic and mechanical properties necessary for the calibration of constitutive models that can reproduce the undrained softening underlying the flow liquefaction phenomenon that caused the dam failure. Specific characteristics of undrained anisotropic behaviour of these heavy iron ore tailings were observed: (*i*) loose specimens tested at low-stress levels and under undrained shearing have a strong strain-softening behaviour, followed by a loss of stability, rapid increase in shear strains and pore pressure development that lead to uncontrollable failure; (*ii*) the peak strength points for these samples allowed the definition of the instability line in the invariant q–$p´$ space (S_p ratio). After the peak undrained strength is mobilised, the stress-path drops down to the critical state loci (CSL) for very low values of q (residual undrained strength, $S_{u,res}$ = q_{res}/2; also designated post-liquefaction strength $S_{u,Liq}$). The normalised strength ratio of the maximum deviatoric stress with the corresponding mean effective stress (S_p=q_{peak}/$p´$) may depend on the consolidation path, although this varies in the literature. However, the normalised strength ratio of the maximum deviatoric stress with the initial (at rest condition) vertical effective stress (S_{p_Ko}=q_{peak}/$\sigma´_{v0}$) does depend on consolidation state (therefore K_0) emerging much larger values of S_{p_Ko} for anisotropic consolidation. This will be discussed below with the data accumulated in recent extensive laboratory tests on tailings in UPorto and is associated with the axial strain required to reach peak strength was much smaller for anisotropic tests (i.e., 0.06%) than for isotropic tests (e.g., 0.90%).

2. Susceptibility: which and why materials "flow" liquefy

This is an undrained process that can be static or cyclic, but can also be induced by a drained process, that can increase the pore pressure by a consistent drop on the mean effective stress with constant deviatoric stress (this is a response known from the very early days of Soil Mechanics – Figure 1).

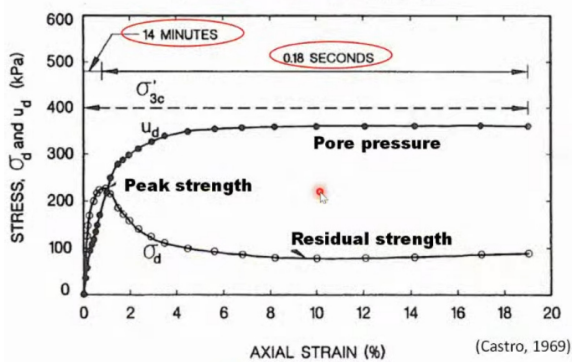

Figure 1. Load control undrained tests results of a granular soil with extreme brittle behaviour

The post-liquefaction/softening undrained strength, which is still diversely designated as a steady state, is the end of a non-Newtonian flowing process, ending in a very low deviatoric stress ($q_{res\approx}=S_{u,res}$):

– will lie on the effective stress frictional failure envelope, so it converges to CSL;
– It has a fundamental characteristic, less dependent on the stress path and fabric.

In Figure 2 the point indicated as "CS" is an ultimate ("residual") deviatoric stress (2 times undrained shear strength) that will be "catch" in very low values the Critical State Line (also known as Critical State Loci).

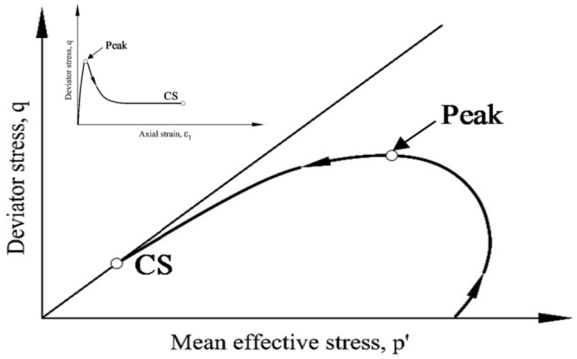

Figure 2. Undrained tests in full or partially full saturated soils

Critical State Soil Mechanics is fundamental to understand where the stress paths come to a residual strength value ($S_{u,res}$ or $S_{u,liq}$) in a stress-space, limited by conditions of a purely frictional behaviour, with constant stress invariants and volume, in constant rate of shear strain. This implies that in an element test, the stress-path will converge for critical state locus (CSL), and all element tests should assure the necessary procedures to allow as much as possible the uniform cylindric shape of the tested specimens and a necessary coaxially of the loads and the principal planes (see recommended procedures in Viana da Fonseca et al. 2021). Figure 3 shows the details that are part of the best procedures to guarantee representative element tests.

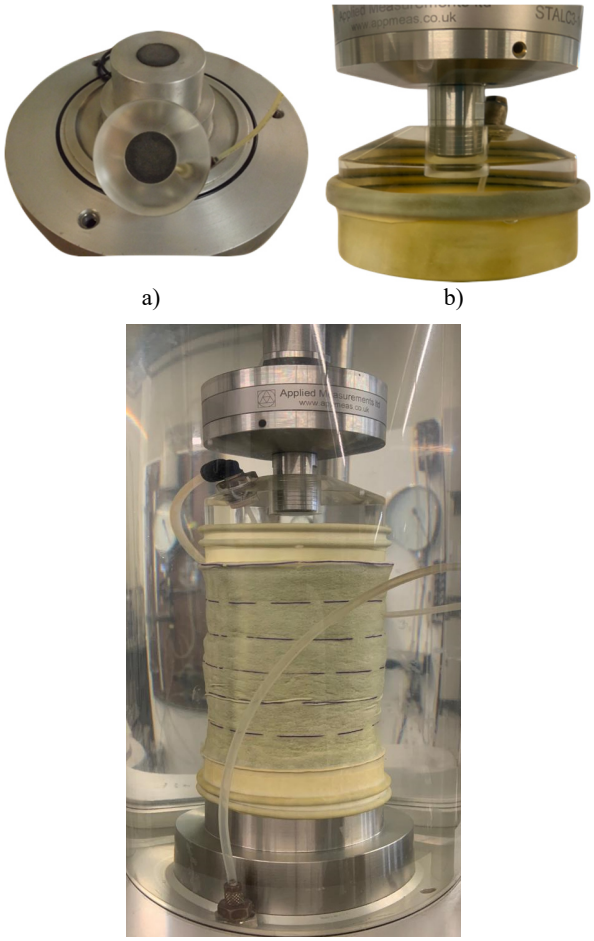

Figure 3. Experimental procedures to guarantee representative element tests (after Viana da Fonseca et al. 2021): a) oversized lubricated end platens; b) embedded top cap loading ram connection; c) aspect of soil specimen after testing

Critical State Soil Mechanics has a fundamental approach to get $s_{u,res}$ ($s_{u,Liq}$) controversial due to:

- its association to limit equilibrium analyses, which can be a misleading of what is a progressive failure and what is really a drop down to residual of a single element itself;
- there may be some confusion since the concepts of post peak (or yield) sensitivity (as in clays) or fragility in sandy/silty soils versus full liquefaction in non-plastic granular soils that are due to cyclic actions where a steady rising of the pore-pressure ratio towards a complete loss of contact between particles (r_u=1, occurs); in this situation frictional strength will not be mobilised when p' is zero.

Monotonic flow liquefaction, mainly in TSF, stands for the drop down to the CSL, after reaching specific instability stress state with rapid deformations (even with constant deviatoric stresses) converging to pure "frictional" state with very low p' and q stresses under undrained conditions (see Figure 4).

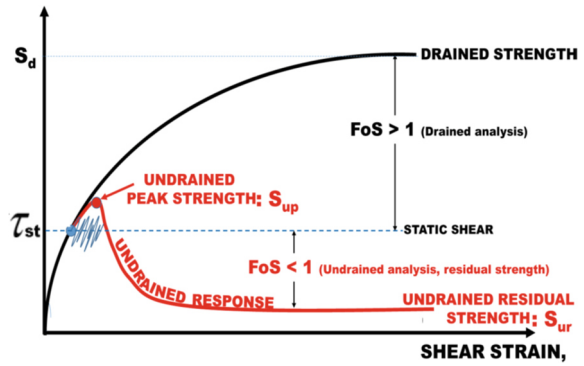

Figure 4. Concept of static liquefaction (Verdugo 2022)

The initial condition necessary for triggering a flow is directly related to the staring level of the static shearing stress, which has to be greater than the minimum undrained strength ($S_{u,res}$). This explain why some authors (e.g., Verdugo 2022) emphasise the fact that if the static shear does not exceed the undrained residual strength, a flow failure cannot be triggered (except migration of water from one sector to another –a decisive factor in the failure of Dam 1 in Brumadinho). However, when the CSL is highly curved, the undrained residual strength for a wide range of mean effective stress is close to zero; for instance, for the tailings studied by Viana da Fonseca et al. (2022b) the undrained residual strength is close to zero is low for stresses lower than 750 kPa. Hence, in this specific case the initial condition necessary for triggering a flow liquefaction is often verified.

Triaxial drained and undrained triaxial tests are useful to evaluate the hydro-mechanical behaviour of materials that develop flow liquefaction under specific mechanisms involved in this kind of fragility. In Figure 5, mechanisms are illustrated with the association of idealized stress paths, where the soil reaches the $S_{u,peak}$, (softening premise) and then converge to the $S_{u,res}$ located at the CSL.

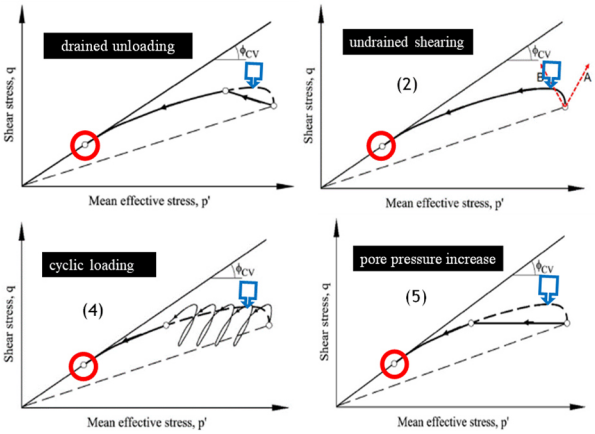

Figure 5. Idealised stress paths associated with liquefaction triggering mechanisms (adapted from Gens 2019)

3. Materials and methods

3.1. The tested iron ore tailing

On January 25th of 2019, the tailings Dam I at the Córrego do Feijão iron mine complex, located in Brumadinho (Minas Gerais, Brazil), suddenly failed, resulting in a catastrophic mudflow that killed hundreds and caused vast economic, social, and environmental repercussions. The dam's failure was unique as it was sudden and abrupt, with no apparent signs of distress prior to the failure. Technical investigations on the causes of failure were commissioned to CIMNE Computational Centre in Polytechnical University of Catalunya (in consortium with the University of Porto). The geotechnical characterisation of the tailings was deemed essential to obtain a credible computational model of the failure; therefore, an extensive sampling and laboratory testing campaign took place (details of this programme can be found in Viana da Fonseca et al. 2022a). FEUP post-mortem campaign identified a set of ideal materials to be representative of the different tailing materials within the dam, that is, types 1, 2, 3 and 4. However, the material Type 4, very similar one of the clusters dominating the failure (Type 3), that is, a CSL highly curved and a very heavy particles density. However, the fine content is rather different, in soil Type 4 is 36%, whereas the fines content in tailing Type 3 is of about 70%. The tailing type 4 was not included in the dam's modelling, as it was still being tested at the time.

The present paper discloses some of the extensive and advanced laboratory program undertaken afterwards to investigate the tailing Type 4. This silty-sand iron tailing was considered an ideal material given its brittleness and site proximity to the initial failure surface location. The tests results comprised evaluations of the physical, hydraulic, and mechanical properties. The test results allowed for the definition of fundamental parameters for the inputs of appropriate constitutive models based in Critical State Soil Mechanics (CSSM) and capable of reproducing a wide range of soil behaviour, from ductile to very brittle, especially the undrained softening underlying the flow liquefaction phenomenon. This is described in Viana da Fonseca et al. (2022b), with emphasis to the procedures to prepare the specimens in its in situ grading.

The material was classified as a non-plastic silty-sand iron tailing. The specific gravity of 4.99 is an uncommonly high value, reflecting the large amount of iron remaining in the processed tailing. Scanning electron microscope (SEM) images were taken to qualitatively assess particle structure, shape, and other parameters at the microscopic level (see Figure 6).

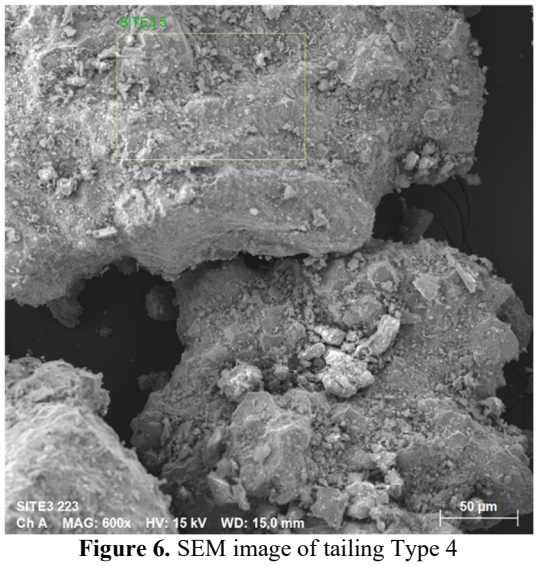

Figure 6. SEM image of tailing Type 4

The imaging indicates subangular to angular particles, with small fibrous particles adhering to the surface of others of much larger dimensions, but they give no indication whatsoever of interparticle bonding. The grain size distribution parameters and physical properties of this tailing are summarised in Table 1.

Table 1. Physical properties of the tailing Type 4

Parameter		Value	Unit
Specific Gravity	G_s	4.994	-
Mean Particle Size	D_{50}	0.093	mm
Fines Content	FC	36.49	%
Coefficient of Curvature	C_c	1.18	-
Coefficient of Uniformity	C_u	3.18	-
Plasticity Index	PI	N.P.	%
Maximum Void Ratio	e_{max}	1.22	-
Minimum Void Ratio	e_{min}*	0.48	-
Particle Shape	Sub-angular to angular		

* value estimated from proctor tests

3.2. Experimental Methodology

The flow liquefaction failure in Brumadinho's dam was a consequence of undrained brittleness of the tailings, a condition of contractive material in which undrained shearing goes through a peak before attaining critical state conditions at much lower stresses. Therefore, the constitute model selected to represent the tailing brittle behaviour was a key feature to simulate flow liquefaction. Critical state soil mechanics (CSSM) offers a clear framework to understand static liquefaction and formulates constitutive models that reproduce this behaviour. In the analyses of the referred panel, the decision was to use the modified version of the Clay and Sand Model (CASM) (Yu 1998) for the modelling of the tailings with some extra improvements described in the technical report by Arroyo and Gens (2022). The experimental program was designed to include laboratory tests (as described in detail in the annex included in that report), which would determine the necessary parameters for the calibration of the constitutive models (Viana da Fonseca et al, 2022a). Oedometer tests were carried out with different initial void ratios (e_0) to examine the potential transitional behaviour of the tailing. Transitional soil behaviour is characterised by non-unique One-Dimensional Normal Compression Line (1D-NCL) and Critical State Locus (CSL), which are incompatible with critical state soil mechanics. The compressibility of the material was also investigated through triaxial tests with several isotropic loading stages, as the compressive nature of the soil can dictate the development of large positive pore pressures that lead to flow liquefaction. This triaxial configuration included Bender Elements (BE), which allowed the estimation of elastic shear modulus to be obtained from shear wave velocity measurements throughout all stages. In addition, permeability values for different effective stresses and void ratio conditions were also obtained from the same triaxial test. In the new samples of the new site – Type 4 – all these tests were conducted, which allowed deriving innovative conclusions that have been enriching the knowledge on these very complex geomaterials.

A proper consideration of the undrained behaviour of the tailing should rely on tests that adopt the initial stress state representative of the in-situ conditions ($K \neq 1$) and specific stress loading paths occurring in the geotechnical structures. A series of anisotropically consolidated undrained tests were carried out on loose and dense samples to evaluate the liquefaction, strain softening and strain hardening behaviour of the tailing. The correct characterisation of the undrained peak strength is of the utmost importance in the context of stability computations, as it signals the onset of instability. The influence of anisotropic consolidation on the yield undrained strength of compression tests was investigated, by testing samples with different K values of 0.5, 0.7 and 1.0. Finally, several drained and undrained extension tests were carried out on loose and dense anisotropically consolidated samples to evaluate the tailings strength parameters in extension conditions. Some of these soil tests are presented in Viana da Fonseca et al. (2023), hereby complemented with additional data.

4. Geomechanic parameters

4.1. Compressibility

One-dimensional tests were carried out on reconstituted specimens to investigate the iron tailing compressibility and transitional mode. To complement the compressibility data, two isotropic compression triaxial tests were carried out in loose samples. Table 2 summarises the compressibility parameters obtained from the tests previously detailed.

Table 2. Compressibility parameters

Test	e_0	λ	κ	λ/κ
Isotropic triaxial	1.24	0.049	0.005	0.10
Isotropic triaxial	1.26	0.070	-	-
Oedometer	1.30	0.095	0.007	0.07
Oedometer	1.10	0.095	0.007	0.07
Oedometer	0.91	0.027	0.006	0.22
CSL	-	0.096	-	-

λ does not refer to a unique normal compression line but represents the gradient of a family of parallel curves. The mean effective stress (p') reached in isotropic triaxial tests is lower than the one achieved in oedometer and critical state. Denser specimens presented a much stiffer behaviour and a well-defined yield point cannot be detected. Moreover, the elastic modulus κ was evaluated through a series of loading and unloading steps. It should be noted that in oedometer tests, κ values increase for the unloading performed at the highest stress. This may signal an evolution in the soil morphology, namely the particle shape or size.

4.2. Critical State

The critical state locus (CSL) of any soil is independent of its initial stress state and its void ratio, thus representing an 'ultimate and stable state' and can

be estimated from laboratory triaxial tests. The results allow obtaining the shear-confinement-volume state, represented by three-dimensional invariants in the e–p'–q plane (void ratio, mean and deviatoric effective stresses). The definition of CSL for each type of tailings of the first campaigns in Dam 1 post-morten, as described in Viana da Fonseca et al. (2022a), was carried out by performing a set of triaxial tests in drained and undrained conditions. The details of the procedures and results of these tests in soils type 1, 2 and 3 were well discussed in that paper, namely some evolution of the position in the CSL compressibility e–ln p' space, when pressures increase which is associated to morphology changing. Figure 7 resumes those results, while Table 3 resumes the state parameters.

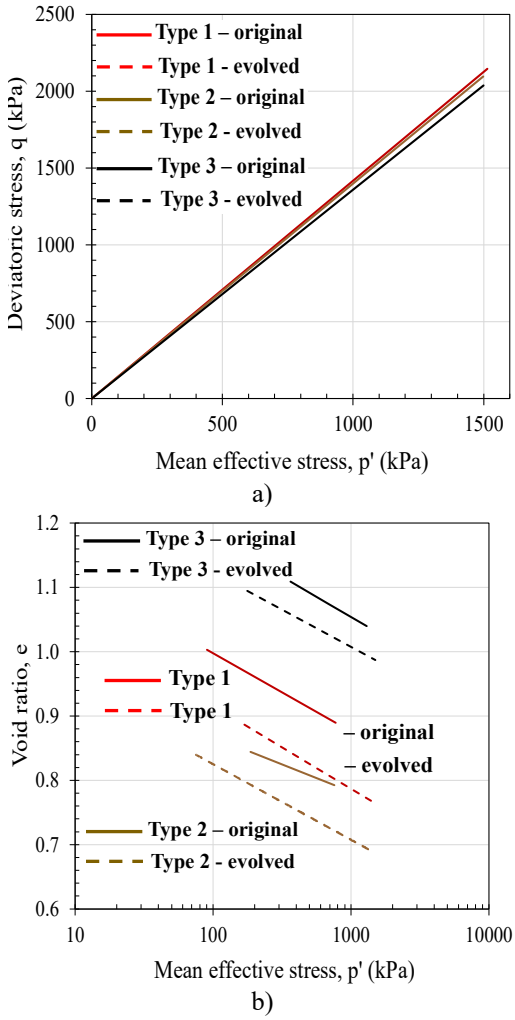

Figure 7. CSL of the three types of tailings in natural and evolved conditions: a) p'–q space; b) e–ln p' space

Table 3. Critical state parameters for the three tailings soil types

Material	Condition	ϕ'_{cs} (°)	M_c (-)	λ_e (-)	Γ (-)
Type 1	Original	35.0	1.42	0.053	1.24
	Evolved			0.056	1.17
Type 2	Original	34.5	1.40	0.037	1.04
	Evolved			0.051	1.06
Type 3	Original	33.6	1.36	0.054	1.43
	Evolved			0.050	1.35

Note that λ_e represents notation in natural logarithm

The evolution of the soil behaviour caused additional compressibility – represented by a shift down of CSL in the e - log p' space. However, it did not affect the friction angle of shearing resistance at the critical state. Such an evolution was attributed to changes in the morphology of soil particles, while grain size distribution after triaxial testing under distinct pressures were similar.

Drained and undrained triaxial tests were also conducted in soil specimens of tailing Type 4 to characterise the CSL. The results of all drained and undrained loose triaxial tests considered to have reached the critical state were used to define the critical state parameters of the tailing in study, observed in Figure 8.

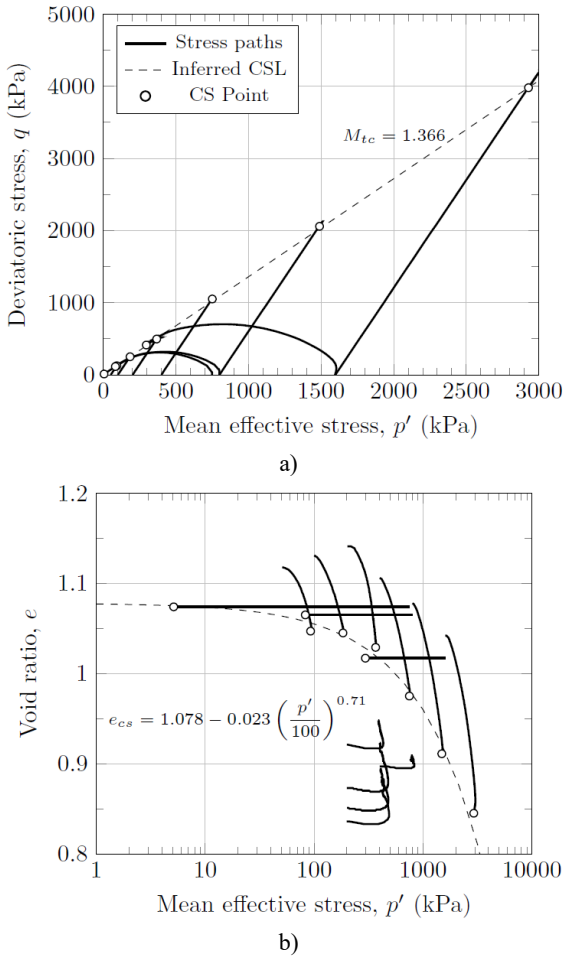

Figure 8. Inferred CSL of tailing Type 4 (after Viana da Fonseca et al. 2022b): a) p'–q invariant space; b) e – ln p' invariant space

The stress-dilatancy relationships of the soil in study were obtained from a set of drained triaxial tests on dilative samples with distinct state parameters (interpretation in Viana da Fonseca et al., 2022b).

Due to the high instability of the tailing Type 4, the CSL in the e – ln p' invariant space can be approximated using a power law relationship as follows:

$$e = A - B\left(\frac{p'}{p_{ref}}\right)^{C} \quad (1)$$

where A, B and C represents three material constants while p' and p_{ref} are the mean effective stress and reference stress condition, respectively. The CSL projection in the in the q–p' space define a strength

parameter M_{tc} equal to 1.366 and a friction angle of shearing resistance of ϕ'_{cs} of 33.8º.

Physical properties of this soil (Type 4) and Type 3, from the previous study were close, although the new sample is coarser (a silty-sand) when compared to the previous (a sandy-silt), but in what respects to colour, iron content and, consequently, the particle density high values as the hydraulic conductivity.

In this new tailing, the compressibility and CSL have higher sensitivity to the variation of the state, that is, a stronger non-linearity stress-states and stress-paths (in compression and extension shearing). This is well seen in Figure 8, with emphasis to the clear nonlinearity of CSL. In the first parametric evaluation (Viana da Fonseca et al., 2022) that line was assumed linear, as a simplification for the calibration of the parameters in CASM model used for the numerical simulation. That hypothesis was considered in view of the stresses that were involved in the main volume affected by the failure mechanism of Dam 1. These were limited in a range of around 100kPa and 1MPa (shaded area in Figure 9), where the quasi-linear CSL may be acceptable at those stress levels. New analyses should consider this non-linearity for any other extra analyses involving different stress levels.

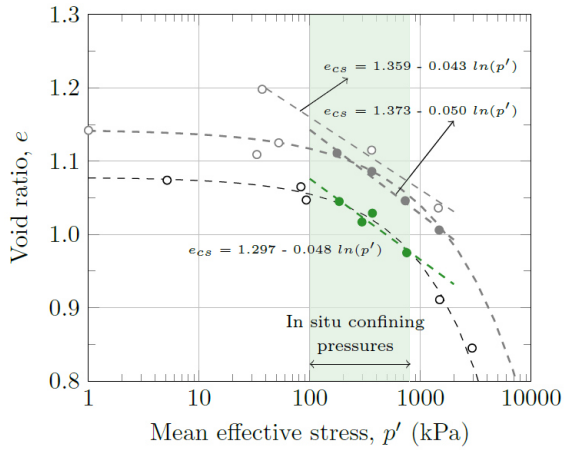

Figure 9. Comparisons between CSL (after Viana da Fonseca et al. 2023)

5. Undrained anisotropic behaviour

5.1. Description of the tests and results

The typical undrained behaviour observed in a non-plastic soil is ruled by the combination of density and stress levels. At lower stress levels, undrained shearing on loose specimens will present a strain-softening compressive behaviour, followed by a loss of stability, rapid increase in shear strains and pore pressure development that can lead to uncontrollable failure. The term instability describes a deformation that occurs due to the inability of a soil specimen to sustain a given load or stress. The instability mechanisms will be distinguished accordingly to (Yamamuro and Covert 2001): (*i*) strain-softening for the reduction of shear strength with increasing strain once the deviatoric stress reaches a peak (q_{pk}); and (*ii*) true liquefaction if that behaviour is so pronounced that the pore pressure equals the confining one, and therefore p' and q tends to zero.

Monotonic effective stress defines a region in the q-p' plane that controls the onset of soil collapse, or better, instability. The maximum shear strength (peak for some, yield for others) locus established in q-p' and e-p' plane define the limit that triggers soil collapse, a function of void ratio. For testing starting undrained after the stress-path had already overpassed the instability line (η_{IL}), will instabilize immediately (see Figure 10).

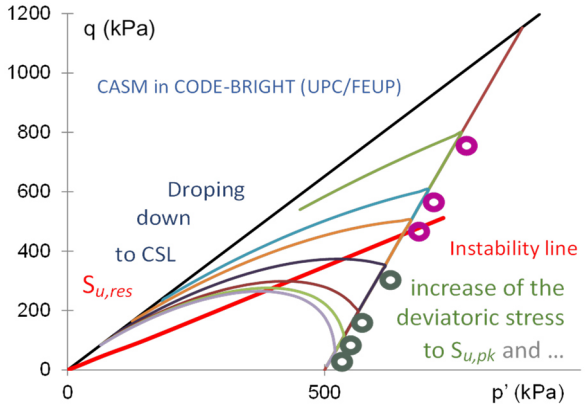

Figure 10. Numerical simulations of Drained-Undrained CK stress-paths in a liquefiable sand (adapted from (Ramos, et al. 2015)

If a test starts to be undrained before reaching the instability line, it follows a typical undrained stress-path, with increase of the deviatoric stress while the effective mean stress decreases. As the drained to undrained process occurs at different steps, the p'_0 value for each simulation varied and so the final point of each stress-path is different. The highest mobilised shear stress, before "softening" (Yield/maximum Undrained Strength), coincides with the intersection in η_{IL}. The final point of each stress-path falls into the CSL. That will be the equivalent undrained residual strength.

In the programme that was developed in geotechnical laboratory of FEUP for the characterisation of the iron ore tailings when loaded under rapid conditions enough to induce undrained behaviour, which in the case of the collapse of Dam 1 in Brumadinho, turned to develop a very fast failure in flow liquefaction (Arroyo and Gens 2021; Viana da Fonseca et al. 2021) – available at http://www. mpf.mp.br/mg/sala-de-imprensa/docs/2021/relatoriofinal-cinme-upc-1.

A fully automated Bishop-Wesley triaxial cell (Cordeiro et al. 2022) was used to identify the hydro-mechanical constitutive parameters necessary as inputs for the model used in the later report (CASM) as described in the appointed link and resumed in Viana da Fonseca et al. (2022b). That system is essential to conduct advanced testing under a numerous of loading strain and stress paths. The samples were remoulded using the techniques described in Viana da Fonseca et al. (2021). For stress-path tests, the samples were 50 mm in diameter with an initial height-to-diameter ratio of $H/D \approx 2$. A full saturation condition with B-values higher than 0.98 was achieved applying the same procedures as in the tests performed to reach ultimate critical state. The importance of full saturation is even more pronounced in undrained tests since the development of pore-water pressure strongly depends on the compressibility of the

pore fluid. In the tests for the first phase that were published in Viana da Fonseca et al. (2022a), the samples were anisotropically consolidated under a K≈0.5 and sheared under undrained stress-strain-controlled paths and could be confronted with isotropic consolidated tests (K=1.0). Hereby, some results of the three soils described above are presented in Figure 11, in q-p' (deviatoric stress vs mean effective stress) giving emphasis to their high sensitivity/fragility. In those plots a SEM photo of each of these soils is included to illustrate the morphology.

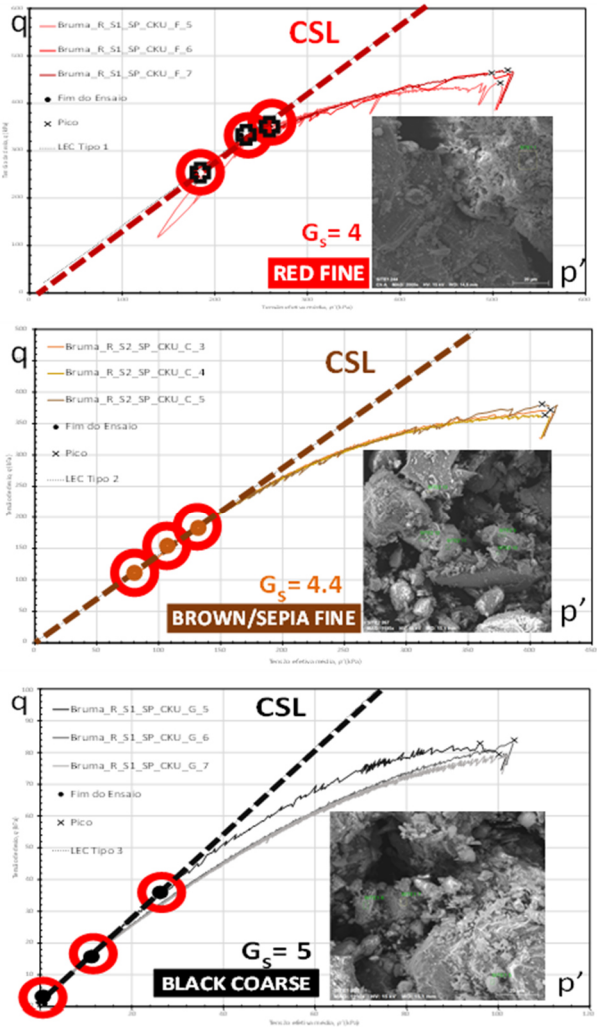

Figure 11. Undrained paths from K_0=0.5 for three types of tailings in Dam 1

These results reflect a trend of decreasing values of residual or ultimate strength, defined in the intersection of the softening ("liquefying") stress paths towards CSL, due to possible changes in the particles roughness.

On the other hand, the samples were anisotropically consolidated under a K of about 0.5 and 0.7 and sheared under undrained stress-strain-controlled paths. The void ratio was determined by the direct measurement of end-of-test water content (Verdugo and Ishihara 1996), since freezing was not compatible with the equipment. The stress and state paths of the test performed to assess the undrained behaviour are presented in Figure 12.

Loose samples developed positive pore water pressure, revealing a tendency of contractive response over a wide range of confining pressures.

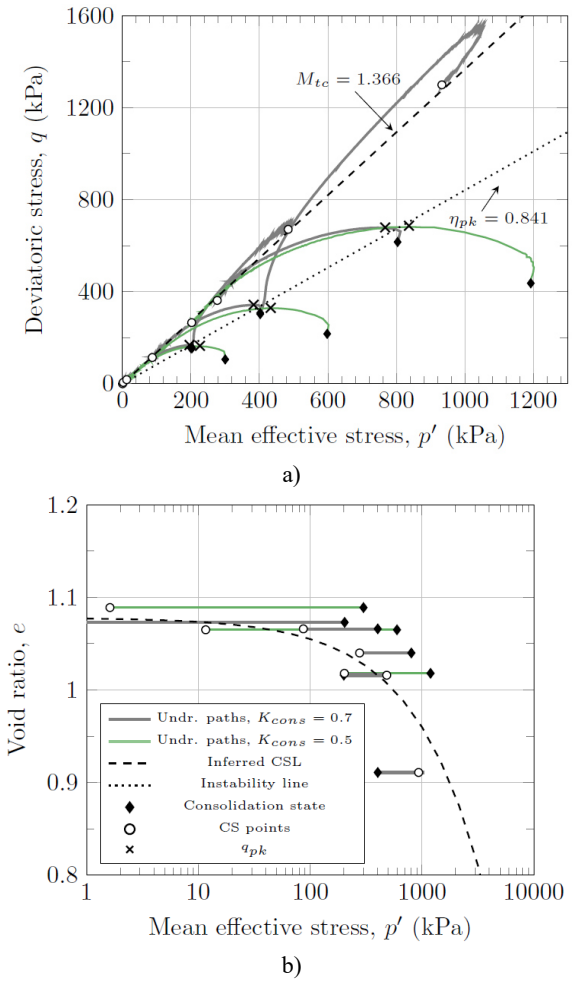

Figure 12. Undrained paths: a) $q - p'$ invariant space; b) e – ln p' invariant space

Tests with mean effective stresses bellow 300 kPa presented true liquefaction, that is, the annulment of the mean effective stress and deviator stress; whereas the other tests presented severe strain softening but with no liquefaction, as a stable critical state was reached. The peak strength points for those samples, which experienced instability mechanisms allowed the definition of the instability line (η_{IL}) in the $q - p'$ invariant space. The stress ratio ($\eta_{pk} = q_{pk}/p'_{pk}$) at which peak is reached was identified in about 0.841. No significant differences were observed between the instability locus for the specimens consolidated under K=0.5 and K=0.7; therefore, only a single η_{IL} was outlined.

5.2. Normalised undrained strength ratio

The point of maximum undrained strength signals the onset of instability and, then, the correct characterisation of peak strength is of utmost importance in the context of stability computations such as those addressing flow liquefaction. The uniqueness of the instability line in the stress space is assumed, as the undrained peak strength for both isotropic and anisotropic (K=0.5 an K=0.7) consolidated tests align on the same linear locus referred in Figure 8 (see Figure 13). The η_{IL} exhibited a slight change from 0.841 to 0.856 after combining the results obtained in both isotropically and anisotropically

consolidated tests, indicating negligible effects of stress-induced anisotropy on soil instability. Such linear criteria have proven useful for limit equilibrium calculations, but they are difficult to implement as calibration constraints in the context of numerical modelling (Mánica et al. 2022).

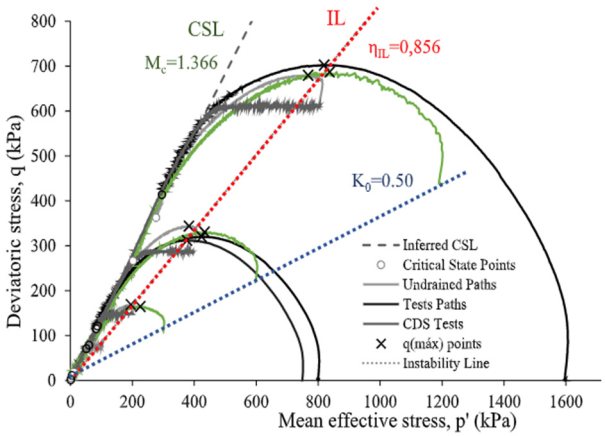

Figure 13. Undrained stress paths in $q - p'$ invariant space for different K values

A stronger calibration constraint is obtained if the undrained peak conditions are characterised through a normalised undrained strength ratio. The normalised undrained strength ratio (S) is typically defined as:

$$S = \frac{s_{u\,pk}}{\sigma'_{vo}} \qquad (1)$$

where $S_{u,pk}$ refers to the peak undrained strength ($S_{u,pk} = q_{pk}/2$) and σ'_{vo} is the consolidation vertical effective stress. From an implementation standpoint, the normalised undrained strength ratio S_p, is preferred. It offers a good description of undrained peak strength in materials exhibiting static liquefaction, and can be defined as:

$$S_p = \frac{s_{u\,pk}}{p'_0} \qquad (2)$$

where p'_0 is the consolidation mean effective stress.

Figure 14 shows the relationships between the undrained peak strength with σ'_{vo} and p'_0 derived from the all the loose undrained triaxial compression tests mentioned referred before. The interesting aspect is that the normalised undrained strength ratio depends on the consolidation path, presenting much larger values of S_p for anisotropic consolidation than for isotropic consolidation.

The level of anisotropy was also reflected with an increasing in S_p values with the decreasing K. The strong influence of consolidation path on the peak undrained strength of this tailing was expected (Fourie and Tshabalala 2005). These authors observed a similar behaviour on the Merriespruit Dam tailings. These authors attributed such behaviour to different fabrics that are created during the different consolidation paths.

The undrained tests featured on Figure 14 also highlighted the undrained brittleness in the tailings. The axial strain required to reach peak strength was extremely small, leading to a rapid strength loss under undrained conditions (i.e., brittle response).

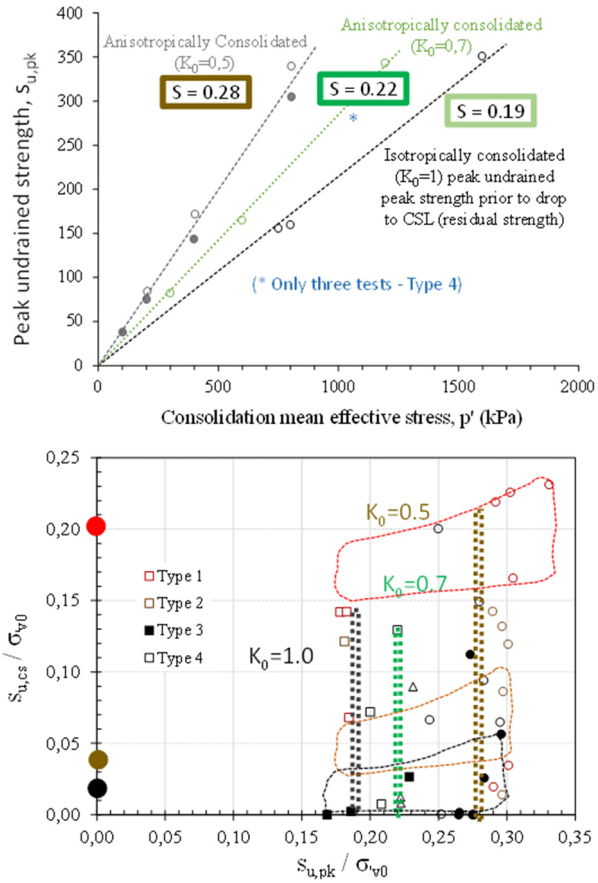

Figure 14. Effect of the consolidation path in consolidation path on the peak and residual undrained strength values

The brittleness index I_B proposed by Bishop (1967) is a soil parameter that would give some insight to the likelihood of a material being involved in a flow slide. It is given by:

$$I_B = \frac{s_{u,pk} - s_{u,cs}}{s_{u,pk}} * 100\% \qquad (8)$$

where $S_{u,cs}$ refers to the critical state undrained strength. As expected, the brittleness index decreases with the increasing compaction or consolidation pressures. However, the I_B index for all the undrained tests was generally greater than 50%, implying a brittle to very brittle behaviour of the soil.

6. Conclusion

This paper has presented an analysis of stress-induced anisotropy in undrained yield and ultimate shear strengths in brittle loose deposited silts, namely iron ore tailings. Experimental results showed that stress-induced anisotropy has negligible effects on the instability locus of the studied tailings. However, the undrained strength ratio $S = s_{u,pk}/\sigma'_{vo}$ can represent well the variation of peak shear strength increases with changes in K (different consolidation conditions), since S is strongly dependent of the anisotropy level. Therefore, the characterisation on these materials under different stress-path is fundamental for the calibration of constitutive models (e.g., CASM), which allows performing numerical studies to assess the stability of tailing storage facilities.

Acknowledgements

Acknowledgements are especially due to Prof. Marcos Arroyo and Prof. Antonio Gens, from CIMNE, who were directly involved in the definition of the lab tests to define the necessary constitutive parameters for the models used in the numerical analyses. This was done under a contract between CIMNE and VALE, SA, under a Term of Cooperation of the Federal Public Prosecutor's Office, (MPF). FEUP, as partner of CIMNE, acknowledges VALE's collaboration in the field and MPF support, namely in the sampling campaigns. This experimental work in FEUP was also part of the research activities of CONSTRUCT– Institute of Research and Development (R&D) in Structures and Construction, funded by national funds through the FCT/MCTES (PIDDAC), with the Base Funding –UIDB/04708/2020.

References

Arroyo, Marcos, and Antonio Gens. 2022. "Computational Analyses of Dam I Failure at the Corrego de Feijao Mine in Brumadinho. Final Report for VALE S.A."

Cordeiro, Diana, Fausto Molina-Gómez, Cristiana Ferreira, Sara Rios, and António Viana da Fonseca. 2022. "Cyclic Liquefaction Resistance of an Alluvial Natural Sand: A Comparison between Fully and Partially Saturated Conditions." *Geotechnics* 2 (1): 1–13. https://doi.org/10.3390/geotechnics2010001.

Fourie, A B, and L Tshabalala. 2005. "Initiation of Static Liquefaction and the Role of K 0 Consolidation." *Canadian Geotechnical Journal* 42 (3): 892–906. https://doi.org/10.1139/t05-026.

Gens, A. 2019. "Hydraulic Fills with Special Focus on Liquefaction." *Proc. XVII European Conference on Soil Mechanics and Geotechnical Engineering*, 1–31. https://doi.org/10.32075/17ECSMGE-2019-1108.

Mánica, Miguel A., Marcos Arroyo, Antonio Gens, and Lluis Monforte. 2022. "Application of a Critical State Model to the Merriespruit Tailings Dam Failure." *Proceedings of the Institution of Civil Engineers - Geotechnical Engineering* 175 (2): 151–65. https://doi.org/10.1680/jgeen.21.00001.

Ramos, Catarina, António Viana da Fonseca, and Jean Vaunat. 2015. "Modeling Flow Instability of an Algerian Sand with the Dilatancy Rule in CASM." *Geomechanics and Engineering* 9 (6): 729–42. https://doi.org/10.12989/gae.2015.9.6.729.

Verdugo, Ramon. 2022. "Static Liquefaction in the Context of Steady State/Critical State and Its Application in the Stability of Tailings Dams." In , 214–35. https://doi.org/10.1007/978-3-031-11898-2_11.

Verdugo, Ramon, and Kenji Ishihara. 1996. "The Steady State of Sandy Soils." *Soils and Foundations* 36 (2): 81–91. https://doi.org/10.3208/sandf.36.2_81.

Viana da Fonseca, António, Davide Besenzon, Fausto Molina-Gómez, Diana Cordeiro, Sara Rios, Bruno Guimarães Delgado, Antônio Mendonça, and Marcos Arroyo. 2023. "Exploring the Uniqueness of Compression and Critical State Lines for Iron Ore Silty-Sand Tailings." *Geomechanics for Energy and the Environment*, under review.

Viana da Fonseca, António, Diana Cordeiro, and Fausto Molina-Gómez. 2021. "Recommended Procedures to Assess Critical State Locus from Triaxial Tests in Cohesionless Remoulded Samples." *Geotechnics* 1 (1): 95–127. https://doi.org/10.3390/GEOTECHNICS1010006.

Viana da Fonseca, António, Diana Cordeiro, Fausto Molina-Gómez, Davide Besenzon, António Fonseca, and Cristiana Ferreira. 2022. "The Mechanics of Iron Tailings from Laboratory Tests on Reconstituted Samples Collected in Post-Mortem Dam I in Brumadinho." *Soils and Rocks* 45 (2): 1–20. https://doi.org/10.28927/SR.2022.001122.

Yamamuro, Jerry A., and Kelly M. Covert. 2001. "Monotonic and Cyclic Liquefaction of Very Loose Sands with High Silt Content." *Journal of Geotechnical and Geoenvironmental Engineering* 127 (4): 314–24. https://doi.org/10.1061/(ASCE)1090-0241(2001)127:4(314).

Yu, H. S. 1998. "CASM: A Unified State Parameter Model for Clay and Sand." *International Journal for Numerical and Analytical Methods in Geomechanics* 22 (8): 621–53. https://doi.org/10.1002/(SICI)1096-9853(199808)22:8<621::AID-NAG937>3.0.CO;2-8.